



## RESEARCH ARTICLE

10.1029/2020JG005810

### Key Points:

- Methane transport from the active layer through groundwater discharge can account for a large fraction of total methane emissions from thaw ponds
- Primary consumers and predators have greater trophic reliance on methane-oxidizing bacteria in ponds with higher methane concentrations
- Increased trophic support by methane-oxidizing bacteria lowers the nutritional quality of pond food chains

### Supporting Information:

- Supporting Information S1

### Correspondence to:

C. Olid,  
olid.carolina@gmail.com

### Citation:

Olid, C., Zannella, A., & Lau, D. C. P. (2021). The role of methane transport from the active layer in sustaining methane emissions and food chains in subarctic ponds. *Journal of Geophysical Research: Biogeosciences*, 126, e2020JG005810. <https://doi.org/10.1029/2020JG005810>

Received 27 APR 2020

Accepted 31 JAN 2021




### Author Contributions:

**Conceptualization:** C. Olid, D. C. P. Lau  
**Formal analysis:** C. Olid, A. Zannella, D. C. P. Lau  
**Funding acquisition:** C. Olid, D. C. P. Lau  
**Investigation:** A. Zannella  
**Project Administration:** C. Olid, D. C. P. Lau  
**Supervision:** C. Olid, D. C. P. Lau  
**Visualization:** C. Olid, D. C. P. Lau  
**Writing – original draft:** C. Olid, D. C. P. Lau  
**Writing – review & editing:** C. Olid, A. Zannella, D. C. P. Lau

© 2021. The Authors.

This is an open access article under the terms of the [Creative Commons Attribution License](https://creativecommons.org/licenses/by/4.0/), which permits use, distribution and reproduction in any medium, provided the original work is properly cited.

# The Role of Methane Transport From the Active Layer in Sustaining Methane Emissions and Food Chains in Subarctic Ponds

C. Olid<sup>1</sup> , A. Zannella<sup>2</sup> , and D. C. P. Lau<sup>1</sup> 

<sup>1</sup>Climate Impacts Research Centre (CIRC), Department of Ecology and Environmental Science, Umeå University, Abisko, Sweden, <sup>2</sup>DISAT, University of Milano-Bicocca, Milano, Italy

**Abstract** Groundwater discharge from the seasonally thawed active layer is increasingly recognized as an important pathway for delivering methane (CH<sub>4</sub>) into Arctic lakes and streams, but its contribution to CH<sub>4</sub> emissions from thaw ponds and its influence on the trophic support and nutritional quality of pond food chains remains unexplored. We quantified the transport of CH<sub>4</sub> from the active layer through groundwater discharge into thaw ponds in a subarctic catchment in northern Sweden, using radon (<sup>222</sup>Rn) as groundwater tracer. We analyzed stable isotopes and fatty acids of pond macroinvertebrates to evaluate the potential effects of groundwater-mediated CH<sub>4</sub> inputs on the aquatic food chains. Our results indicate that active layer groundwater discharge flows are nontrivial (range 6%–46% of pond volume per day) and the associated CH<sub>4</sub> fluxes (median 339 mg C m<sup>-2</sup>day<sup>-1</sup>, interquartile range [IQR]: 179–419 mg C m<sup>-2</sup> day<sup>-1</sup>) can sustain the diffusive CH<sub>4</sub> emissions from most of the ponds (155 mg C m<sup>-2</sup> day<sup>-1</sup>, IQR: 55–234 mg C m<sup>-2</sup> day<sup>-1</sup>). Consumers in ponds receiving greater CH<sub>4</sub> inputs from the active layer had lower stable carbon (C) isotope signatures that indicates a greater trophic reliance on methane oxidizing bacteria (MOB), and they had lower nutritional quality as indicated by their lower tissue concentrations of polyunsaturated fatty acids. Overall, this work links physical (CH<sub>4</sub> transport from the active layer), biogeochemical (CH<sub>4</sub> emission), and ecological (MOB-consumer interaction) processes to provide direct evidence for the role of active layer groundwater discharge in CH<sub>4</sub> cycling of subarctic thaw ponds.

**Plain Language Summary** Global warming in the Arctic leads to thawing of permafrost (soil that remains at or below 0°C for at least 2 consecutive years) and the formation of water-filled depressions known as thaw ponds. Small ponds (areas < 0.001 km<sup>2</sup>) in permafrost regions account for a disproportionately large share of methane emissions from freshwater lakes and ponds worldwide. Predictions for methane emissions in a warmer climate depend on our understanding of the processes that affect the production and accumulation of methane in these systems. This study shows that groundwater flowing through the upper seasonally thawed active layer is an important conduit for transporting methane into thaw ponds. These external methane inputs can sustain methane emissions from the ponds. The effects of active layer groundwater discharge on the net balance between methane inputs and outputs also impacted the thaw pond food chain. Invertebrates in thaw ponds with higher methane concentrations had lower nutritional quality and relied more on carbon and energy from bacteria that oxidize methane. Understanding the role of active layer groundwater discharge in methane cycling of thaw ponds is key for better predictions of climate-change impacts on methane emissions and food chains of these freshwater systems.

## 1. Introduction

Climate warming and shifts in precipitation regimes are particularly strong in arctic and subarctic regions (IPCC, 2013), causing thawing of permafrost and the formation of small water basins (Bouchard et al., 2014; O'Donnell et al., 2012). These thaw (thermokarst) lakes and ponds are ubiquitous in the permafrost landscape and hotspots for carbon dioxide (CO<sub>2</sub>) and methane (CH<sub>4</sub>) emissions (Holgerson & Raymond, 2016; Kuhn et al., 2018; Laurion et al., 2010; Wik et al., 2016). Small ponds (surface areas smaller than 0.001 km<sup>2</sup>) in particular are a major natural source of CH<sub>4</sub>, contributing to 40% of the total diffusive CH<sub>4</sub> emissions from freshwater lakes and ponds worldwide (Holgerson & Raymond, 2016; Kuhn et al., 2018; Wik et al., 2016). Yet, previous studies of CH<sub>4</sub> emissions from thermokarst freshwaters have mainly focused on medium- to

large-sized systems (Walter et al., 2007). By comparison, little is known regarding CH<sub>4</sub> emissions from small thaw ponds and, especially, their environmental drivers.

Concentrations of CH<sub>4</sub> in surface freshwaters are determined by the interplay between CH<sub>4</sub> inputs and losses (Bastviken et al., 2004; Karlsson et al., 2007; Laurion et al., 2010; Rubbo et al., 2006). High CH<sub>4</sub> concentrations in freshwaters are usually ascribed to high CH<sub>4</sub> production rates in anoxic sediments (Bastviken et al., 2004) or in the oxic water column (DelSontro et al., 2018). However, high CH<sub>4</sub> concentrations in freshwaters in permafrost regions can also result from the large supply of externally produced CH<sub>4</sub> through active layer groundwater discharge (Connolly et al., 2020; Dabrowski et al., 2020; Paytan et al., 2015). Here, active layer groundwater discharge flow is defined as the supra-permafrost groundwater flow that circulates through the unfrozen zone of the active layer due to the hydraulic gradient and discharges into surface waters. The active layer groundwater flow is CH<sub>4</sub>-rich and accounts for a large fraction of CH<sub>4</sub> emissions from lakes and streams in permafrost regions (Dabrowski et al., 2020; Kling et al., 1992; Lecher et al., 2017; Paytan et al., 2015). While climate change is expected to have profound influences on the hydrology of the Arctic by reducing the permafrost extent and increasing the thickness of the active layer (Vihma et al., 2016; Woo et al., 2008), little information is available on the overall transport of CH<sub>4</sub> from the active layer into thaw ponds. Thus, estimating the importance of active layer groundwater discharge on CH<sub>4</sub> emissions from thaw ponds is crucial for understanding the role of small ponds in the global carbon (C) cycle and for better predict future climate feedbacks.

While lateral groundwater flow paths may be important sources of CH<sub>4</sub>, oxidation of CH<sub>4</sub> at oxic-anoxic interfaces in the sediment and water column by methane oxidizing bacteria (MOB) is a major constraint to CH<sub>4</sub> emissions from freshwaters (Bastviken et al., 2002). In turn, MOB can serve as a basal resource that supports aquatic food chains, providing energy and C to both benthic and pelagic consumers (Jones & Grey, 2011; Jones et al., 2008; Lau et al., 2014). In particular, chironomids (Diptera: Chironomidae) are abundant in aquatic ecosystems and can consume significant amounts of MOB as a supplement to other basal resources (e.g., algae and terrestrial organic matter) during their larvae stage (Jones et al., 2008). Chironomids are prey for many aquatic predators including fish, and are key players in transferring biogenic CH<sub>4</sub> from MOB to freshwater food webs (Jones & Grey, 2011). Yet, MOB have lower nutritional quality compared to algae, as MOB are unable to biosynthesize polyunsaturated fatty acids (PUFA, e.g., eicosapentaenoic acid and docosahexaenoic acid) which are essential for animal growth and reproduction (Taipale et al., 2012). Hence, increased CH<sub>4</sub> oxidation and trophic support by MOB can potentially result in lower production and nutritional quality (i.e., PUFA content) of aquatic consumers. To the best of our knowledge, no study has investigated simultaneously the net effect of active layer groundwater discharge on the CH<sub>4</sub> cycling and the trophic support and nutritional quality of consumers in thaw ponds.

The purpose of this study was to assess the magnitude of active layer groundwater flows discharging into small thaw ponds, and evaluate its importance for CH<sub>4</sub> emissions and support of food webs. The natural occurring radioactive isotope radon (<sup>222</sup>Rn) was used as groundwater tracer. Stable C and nitrogen (N) isotopic signatures ( $\delta^{13}\text{C}$  and  $\delta^{15}\text{N}$ ) of primary consumers (chironomid larvae) and their predators (Coleoptera: Dytiscidae) were used to evaluate how changes in pond CH<sub>4</sub> budgets related to groundwater inputs from the active layer would affect the trophic reliance on MOB and the nutritional quality of the animals. We predicted that groundwater-mediated CH<sub>4</sub> inputs from the active layer would sustain the CH<sub>4</sub> emissions from the thaw ponds. As higher concentrations of CH<sub>4</sub> are expected to enhance activities and production of MOB (Bastviken et al., 2003), our second prediction was that the trophic reliance of chironomid larvae and dytiscid beetles on MOB would be greater in ponds with higher CH<sub>4</sub> concentrations in relation to greater groundwater discharge from the active layer. Also, as MOB have lower food quality (i.e., PUFA content) compared to algae, we expected that the tissue PUFA concentrations of consumers would be lower with increasing trophic reliance on MOB (as indicated by lower  $\delta^{13}\text{C}$  of the consumers).

## 2. Materials and Methods

### 2.1. Study Area

The study was carried out in the Stordalen catchment (68°20'90"N, 18°58'57"E), a 15 km<sup>2</sup> peatland complex located at about 10 km east of Abisko in northern Sweden. The catchment is in the sporadic permafrost

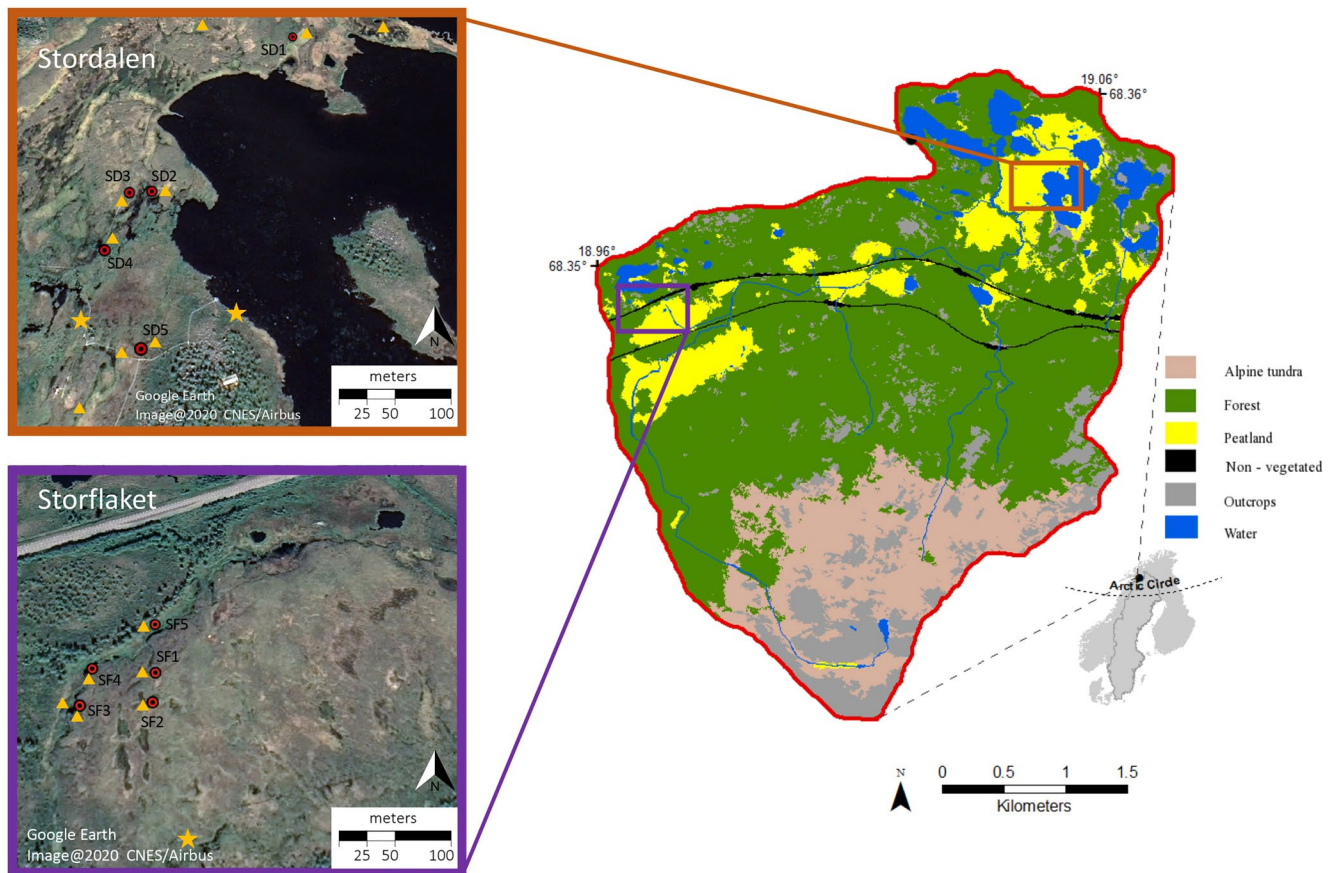


**Figure 1.** The Stordalen catchment, east of Abisko at the Torneträsk catchment, Swedish Lapland. Red dots indicate the location of the study ponds. Yellow symbols indicate the location of groundwater wells (stars) and bores (triangles) (Modified from Lundin et al., 2016).

zone and permafrost is mainly found above 800 m a.s.l. (Gisnås et al., 2016) but also exists in peat mires and exposed areas at lower elevations (Åkerman & Johansson, 2008). The total annual precipitation was 304 mm in 1961–1990 (Alexandersson et al., 1991) and increased since then to 362 mm in 1997–2007 (Abisko Station meteorological data; [www.polar.se/abisko](http://www.polar.se/abisko)). The region has warmed 1.5°C in recent decades, from a mean annual air temperature of  $-0.9^{\circ}\text{C}$  in 1974 to  $0.6^{\circ}\text{C}$  in 2006 (Callaghan et al., 2010), causing rapid thawing of permafrost, shallow water pool formation, and changes in vegetation cover (Åkerman & Johansson, 2008; Johansson et al. 2006, 2013; Malmer et al., 2005).

The two study mires, Storflaket and Stordalen, are located within the Stordalen peatland complex (Figure 1). At both mires, the thickness of the active layer in late September is around 0.5–1.0 m in the raised plateaus and between 1–3 m in the hollows (Åkerman & Johansson, 2008; Klaminder et al., 2008). Storflaket is characterized by a peat palisa plateau with a peat layer of 0.6–0.9 m thick and a water table depth around 0.3 m in October 2013 (Åkerman & Johansson, 2008). Dominant vegetation consists of peat moss (*Sphagnum* spp.), *Eriophorum vaginatum* L., *Vaccinium vitis-idaea* L., *Andromeda polifolia* L., *Betula nana* L., *Empetrum nigrum* L., and *Rubus chamaemorus*. The Stordalen mire is a partially degraded palisa system with an average peat depth around 0.5 m, but with large local variation. The topography is controlled by permafrost heave, with uplifted palsas with permafrost, thawing lawns with thermokarst ponds, and permafrost-free, water saturated fens. The mire is bordered by postglacial lakes on its western, northern, and eastern edges. Accordingly to Olefeldt and Roulet (2012), the mire can be divided in three peatland types: a central bog that drains southward into the south fen, surrounding palsas that can drain to the bog or into surrounding fens and lakes, and fens on southern and northern parts of the mire that receive water from the lake to the east. Hummocks are mainly dominated by nutrient-poor vegetation such as dwarf shrubs (*Empetrum hermaphroditum*, *Betula nana*), lichens (*Cladonia* spp), and mosses (*Sphagnum fuscum*, *Dicranum elongatum*).

Vegetation in the hollows is mainly composed of graminoids such as *Carex rostrata* and *Eriophorum angustifolium*, indicating the minerogenic conditions resulted from nutrient inputs via groundwater flows. A more detailed description of the hydrology and vegetation of the mires can be found elsewhere (Johansson et al., 2013; Malmer et al., 2005; Olefeldt & Roulet, 2012).

## 2.2. Conceptual Model for Estimating Active Layer Groundwater Discharge Using Radon ( $^{222}\text{Rn}$ )

Active layer groundwater flow discharging into the ponds was estimated using a radon ( $^{222}\text{Rn}$ ) mass balance approach (Dabrowski et al., 2020; Dimova et al., 2013). Radon (Rn, hereafter) is a radioactive (half-life of 3.8 days) noble gas that is produced from the radioactive decay of  $^{226}\text{Ra}$  (Ra, hereafter), which occurs ubiquitously in rocks, soils, and sediments and, to a lesser extent, by decay of dissolved Ra. Radon can emanate from Ra bearing minerals and, subsequently, enter the groundwater and be transported through the aquifer. Radon is a useful tracer for quantifying groundwater discharge because it is typically enriched when compared to surface waters. The Rn mass balance approach assumes that: (1) Rn concentrations in the ponds are representative of the average Rn concentrations over days to weeks; (2) the only significant Rn source in pond waters is groundwater inflows from the active layer and pond sediments, and to a lesser extent Ra production in the water column; and (3) the only losses of Rn are due to radioactive decay and atmospheric evasion. The mass balance model for Rn concentrations in a pond system can thus be described by:

$$\frac{\partial \text{Rn}_{\text{pond}} V}{\partial t} = Q_{\text{gw}} \text{Rn}_{\text{gw}} + \lambda V \text{Ra} + F_{\text{diff}} A - F_{\text{atm}} A - \lambda V \text{Rn}_{\text{pond}} \quad (1)$$

where  $\text{Rn}_{\text{pond}}$  and  $\text{Rn}_{\text{gw}}$  are the Rn concentration ( $\text{Bq m}^{-3}$ ) in pond water and active layer groundwater, respectively;  $Q_{\text{gw}}$  is the volume of groundwater discharging from the active layer ( $\text{m}^3 \text{day}^{-1}$ ); Ra is the Ra concentration in pond water ( $\text{Bq m}^{-3}$ );  $F_{\text{diff}}$  is the net diffusive flux of Rn per unit area from underlying sediments ( $\text{Bq m}^{-2} \text{day}^{-1}$ );  $F_{\text{atm}}$  is the Rn evasion to the atmosphere ( $\text{Bq m}^{-2} \text{day}^{-1}$ );  $\lambda$  is the radioactive constant of Rn ( $0.181 \text{days}^{-1}$ ); and  $A$  ( $\text{m}^2$ ) and  $V$  ( $\text{m}^3$ ) are the area and volume of the pond, respectively. For steady-state conditions (i.e.,  $\frac{\partial \text{Rn}_{\text{pond}} V}{\partial t} = 0$ ), the flux of groundwater discharging from the active layer ( $Q_{\text{gw}}$ ) can be estimated by the imbalance between Rn sources (sediment diffusion and Ra production) and sinks (atmospheric evasion and radioactive decay).

## 2.3. Sample Collection and Analyses

### 2.3.1. Ponds Waters

Ponds waters were collected from the surface (maximum 0.5 m from the surface) of five ponds in Storflaket (SF1, SF2, SF3, SF4, and SF5) and five ponds in Stordalen (SD1, SD2, SD3, SD4, and SD5) on July 11–12, 2017. Dissolved organic carbon (DOC) samples were collected in acid washed polyethylene bottles and, after filtration (0.45  $\mu\text{m}$  pore-size) and acidification (100  $\mu\text{L}$  of 20% HCl to 50 mL filtrate water), analyzed by high-temperature catalytic oxidation performed on a Shimadzu TOC-V CPH analyzer (Shimadzu Corporation, Japan, mean of coefficients of variation = 5.5%). Dissolved inorganic carbon (DIC) and  $\text{CH}_4$  concentrations were determined by analyzing the headspace of gastight vials (22 mL vials, PerkinElmer Inc., USA), after addition of 50  $\mu\text{L}$  of 4% HCl to a 4 mL water sample, using gas chromatography (Clarus 500, PerkinElmer Inc., USA). Briefly, samples were preheated to a constant temperature (40°C) on the headspace sampler before injection to the capillary column (Elite-Plot Q, 30 m length, 0.53 mm internal diameter). Oven temperature was set to 100°C, and the detector temperature to 250°C. The samples were analyzed on a flame ionization detector (FID), equipped with a methanizer. A gas mixture with known concentrations of  $\text{CO}_2$  (400 and 9,500 ppm) and  $\text{CH}_4$  (10 and 500 ppm) was analyzed as standards together with each batch of samples. Triplicate analyses of the standards were within 2% coefficient of variation.

Partial pressure of  $\text{CO}_2$  was determined in the field using an infra-red  $\text{CO}_2$  detector (Vaisala Inc., Finland). Similarly, dissolved oxygen (DO) concentration was measured at the mid-depth at the deepest point of the pond using a handheld optical portable probe (ProODO, YSI Inc., USA).



For Rn analyses, water samples were collected using a submersible pump. Here, water was directly pumped into 1.5 L polyethylene terephthalate (PET) bottles and left overflowing to replenish the volume at least thrice to ensure minimal contact with air. Shortly after collection, dissolved Rn concentrations were determined using a radon-in-air monitor (DurrIDGE RAD7) coupled to the RAD7 Soda bottle aerator kit (RAD7 setup, hereafter). Concentrations of Rn in water were determined from the measured concentrations of Rn in air by using the air-water partitioning of Rn corrected for water salinity and temperature (Schubert et al., 2012).

To determine the production of Rn supported by its parent nuclide Ra ( $\lambda R_{a_{\text{pond}}} V$ ), large volumes of water (ca. 20–30 L) were collected using a submersible pump and passed through columns loosely filled with MnO<sub>2</sub>-impregnated acrylic fiber (ca. 25 g dry) to quantitatively extract Ra isotopes (Moore & Reid, 1973). The fibers were rinsed with Milli-Q water, burned at 820°C for 16 h (Charette et al., 2001), ground, and transferred into hermetically sealed counting vials. Samples were stored at least three weeks before counting to ensure the equilibrium between Ra and its daughter <sup>214</sup>Pb. Radium content was determined by gamma spectrometry using a high purity Small Anode Germanium (SAGE) well detector (Canberra, Model GSW120).

### 2.3.2. Active Layer Groundwater

Several surveys were conducted to collect groundwater samples from the active layer for analyses of Rn, CH<sub>4</sub>, DOC, DIC, and total nitrogen (TN). Active layer groundwater samples were collected in September 2017 from preexisting boreholes where piezometers were installed (0.7–1.5 m depth) at two different locations within Stordalen and at one location within Storflaket (Figure 1). For Rn analyses, active layer groundwater was collected into 0.5 L PET bottles and measured right after collection using a RAD7 monitor coupled to the gas extraction accessory RAD H2O. Additionally, bores were dug in the active layer close (0.5–1.0 m) to the sampled ponds to a depth of 0.5–1.0 m below surface using a hand saw and a shovel. The bores were purged using a submersible pump for several minutes (at least three bore volumes) to ensure sample quality. Active layer groundwater samples from the bores were collected in glass bottles (250 mL capacity) designed for Rn analyses (WAT-250 system, DurrIDGE Co.). In October 2017, new bores were dug and 10 mL of filtered (0.45 μm) active layer groundwater were directly transferred to 20 mL polyethylene vials prefilled with a 10 mL high-efficiency liquid scintillator cocktail (Cable & Martin, 2008). Concentrations of Rn were analyzed using an ultra-low-level liquid scintillation counter (Quantulus 1220) with alpha-beta discrimination counting (background of 0.02–0.07 cpm; efficiency of 1.5–3.0, depending on the quenching factor of the sample). A last active layer groundwater sampling campaign was carried out in August 2019. Here, groundwater from the active layer was collected using a submersible pump from new bores dug close (0.5–1.0 m) to the sampled ponds into 0.5 L PET bottles and measured using the RAD7 monitor coupled with the RAD H2O accessory. All active layer groundwater samples were analyzed for DOC, DIC, and CH<sub>4</sub> following the methods described above.

### 2.3.3. Radon Equilibration Experiments

Two benthic sediment samples were collected from the edge of two ponds in Stordalen and Storflaket using a shovel and placed in Ziploc bags. Once in the lab, the sediment samples were placed into 0.5 L PET bottles with a known volume of Milli-Q water. The bottles were then measured using the RAD7 setup that ran 48 two-hour cycles. The rate of Rn diffusion from the sediment ( $F_{\text{diff}}$ ) was derived from the linear gradient obtained when Rn concentrations in air were plotted against time for the first seven hours of the experiment (Chanyotha et al., 2014).

Bulk sediments were used for sediment equilibration experiments to obtain the Rn concentration in active layer groundwater (Chanyotha et al., 2014; Corbett et al., 1998). Briefly, ca. 200 g of dry sediment were placed into 0.5 mL PET bottles and the remaining volume filled with Milli-Q water. All bottles were hermetically sealed and stored for 21 days, being periodically shaken. The Rn concentration in water was directly measured using the RAD7 coupled with the RAD7 setup. The Rn concentration in groundwater from the active layer was calculated as:

$$Rn_{\text{gw}} = Rn_{\text{incubation}} \frac{R_{\text{lab}}}{R_{\text{field}}} \quad (2)$$

where  $Rn_{\text{incubation}}$  is the measured Rn concentration ( $\text{Bq m}^{-3}$ ), and  $R_{\text{lab}}$  and  $R_{\text{field}}$  are ratios of volume of water to sediment in the bottle (lab) and in the field (field) (which is a function of the porosity), respectively (Stieglitz et al., 2013).

#### 2.3.4. Ancillary Measurements

Wind speed was measured continuously and logged as 1-h averages. Single measurements of water temperature and salinity were taken in the field below the water surface (at maximum 0.5 m depth) using a hand-held optical portable probe (ProODO, YSI Inc., USA). Conductivity and pH were measured at the Abisko Research Station with pH and conductivity electrodes (MP220, Mettler Toledo International Inc., USA).

#### 2.3.5. Benthic Fauna, Stable-Isotope (SI), and Fatty-Acid (FA) Analyses

Benthic fauna, that is, chironomid larvae and dytiscid larvae and/or adults, were collected by sweeping a kick net (0.5 mm mesh size) along ca. 1 m (duration  $\times$  distance = 30 s  $\times$  1 m) close to the pond bottom at shore habitats. Multiple sweep samplings were conducted to cover different pond shore areas. Individuals were sorted directly after collection and kept in tap water without food at 4°C overnight to allow them to empty their guts. Afterward, samples were stored at  $-20^{\circ}\text{C}$  until analysis. Samples of individual taxa from each pond were pooled to ensure sufficient material for subsequent analyses of FA as well as stable C ( $\delta^{13}\text{C}$ ) and N ( $\delta^{15}\text{N}$ ) isotope analyses.  $\delta^{13}\text{C}$  and  $\delta^{15}\text{N}$  are complementary for trophic investigations:  $\delta^{13}\text{C}$  changes little during trophic transfer from basal resources (e.g., algae and terrestrial organic matter, etc.) to higher trophic levels, thus the  $\delta^{13}\text{C}$  of consumer tissue can reflect that of the major dietary source; while  $\delta^{15}\text{N}$  progressively increases in food chains and can indicate the trophic positions of consumers (Peterson & Fry, 1987). Chironomid and dytiscid samples were freeze-dried (freeze dryer: LyoDry Compact, MechaTech Systems Ltd, Bristol) and pulverized using a mortar and a pestle. Approximately 1.0 mg of each sample was weighed into tin capsules using a microbalance (Mettler Toledo), and analyzed for  $\delta^{13}\text{C}$  and  $\delta^{15}\text{N}$  using an elemental analyzer interfaced to a continuous flow isotope ratio mass spectrometer (PDZ Europa 20-20; Sercon Limited, Cheshire, UK) at the University of California Davis Stable Isotope Facility.  $\delta^{13}\text{C}$  and  $\delta^{15}\text{N}$  (in ‰) were calculated as  $(R_{\text{sample}}/R_{\text{standard}}) - 1$ , where  $R = N(^{13}\text{C})/N(^{12}\text{C})$  or  $N(^{15}\text{N})/N(^{14}\text{N})$ , and  $N$  is the number of isotopes of the specific mass number of C or N. Ratios are relative to the international standards of Vienna PeeDee Belemnite for  $\delta^{13}\text{C}$  and air for  $\delta^{15}\text{N}$ . Instrument precisions estimated via repeated measurements of internal standards for  $\delta^{13}\text{C}$  and  $\delta^{15}\text{N}$  were 0.03‰ and 0.02‰ respectively.

Fatty-acid (FA) composition of macroinvertebrates was analyzed following the methods described in Grieve and Lau (2018). In brief, FA of ca. 5–10 mg dried samples were extracted using 3:2 (v:v) hexane-isopropanol solution and methylated with 1:17:83 (v:v:v) trimethylsilyldiazomethane-isopropanol-dichloromethane solution. Internal standards for FA quantification were deuterium-labeled pentadecanoic acid, deuterium-labeled methyl heptadecanoate, tridecane, and octacosane. Concentrations of the resultant FA methyl esters were analyzed using a gas chromatography-mass spectrometry (7890A GC, Agilent Technologies, CA, United States; PegasusR High Throughput TOF-MS, MI, United States) installed with a DB-5 capillary column (length 30 m, internal diameter 250  $\mu\text{m}$ , film thickness 0.25  $\mu\text{m}$ ; Agilent Technologies). The Supelco 37 Component FAME Mix (Sigma-Aldrich Sweden AB, Stockholm, Sweden) and Bacterial Acid Methyl Ester BAME Mix (Sigma-Aldrich Sweden AB) were used to identify individual FA. Details of the gas chromatography-mass spectrometry methods are described in Grieve and Lau (2018). In each sample, concentrations of individual FA are reported as percentages relative to the total FA concentrations.

#### 2.4. Gas Fluxes to the Atmosphere

Gas evasion to the atmosphere ( $F_{\text{atm}}$ ) depends on molecular diffusion by concentration gradients and turbulence transfer, which can be calculated using the relationship:

$$F_{\text{atm}} = k(C_w - \alpha C_{\text{air}}) \quad (3)$$

where  $C_{\text{air}}$  and  $C_w$  are the gas concentrations in the air and the surface pond water, respectively;  $\alpha$  (dimensionless) is the partitioning coefficient corrected for salinity and temperature (Schubert et al., 2012); and  $k$  ( $\text{m day}^{-1}$ ) is the gas transfer velocity.

Wind-dependent gas transfer velocities ( $k$ ) were estimated from the empirical equation of (Macintyre et al., 1995):

$$k = k_{600} (\text{Sc} / 600)^n \quad (4)$$

where  $\text{Sc}$  is the Schmidt number for the corresponding gas at the desired water temperature ( $\text{Sc}$  is divided by 600 to normalize to  $\text{CO}_2$  at  $20^\circ\text{C}$ ) (Wanninkhof, 2014). The Schmidt number exponent  $n$  was given the value  $-0.5$  for wind speeds exceeding  $3.7 \text{ m s}^{-1}$  and  $-0.75$  for wind speeds below  $3.7 \text{ m s}^{-1}$ .  $k_{600}$  was calculated based on the equation provided by (Cole & Caraco, 1998):

$$k_{600} = 2.07 + 0.215 U_{10}^{1.7} \quad (5)$$

where  $U_{10}$  is the wind speed ( $\text{m s}^{-1}$ ) normalized to a height of 10 m above the water surface.

The  $U_{10}$  was calculated from the measured wind speed ( $U_z$ ) following (Crusius & Wanninkhof, 2003):

$$U_{10} = U_z \left\{ \left[ 1 + (C_{d10})^{1/2} / \kappa \right] \ln(10 / z) \right\} \quad (6)$$

where  $C_{d10}$  is the drag coefficient at 10 m height (0.0013),  $\kappa$  is von Karman's constant (0.41), an  $z$  is the height of the sensor.

To obtain a representative  $k_{600}$  value, we used the hourly data on wind speed during the 24-h period prior sampling. This time period corresponds to the maximum residence time of Rn within a pond, that can be approximated as  $1 / (\lambda + k / h)$  if the role of evaporation is assumed to be negligible (Rodellas et al., 2018, 2020), where  $\lambda$  is the radioactive constant of Rn (0.181 days $^{-1}$ );  $k$  is the gas transfer velocity ( $\text{m day}^{-1}$ ) and  $h$  is the pond mean depth (m). The estimated residence time of Rn was within the range of the residence time of  $\text{CH}_4$  (1.4–2.8 days) for ponds from the same area computed by dividing the amount of  $\text{CH}_4$  stored by the pond mean  $\text{CH}_4$  surface flux from flux chambers (Kuhn et al., 2018). We acknowledge that the results for the residence time of  $\text{CH}_4$  should be considered upper limits since the  $\text{CH}_4$  removal pathway of oxidation is not included in the computation. To consider a stronger effect of degassing on the gases concentrations closer to the sampling time for  $k_{600}$  estimates, we used a weighting factor to the hourly wind speeds data as shown by (Rodellas et al., 2020).

## 2.5. Data Analysis

One-way ANOVA was used to assess if morphological and physicochemical characteristics of the ponds significantly differed between mires ( $p < 0.05$ ). We used principal component analysis (PCA) to examine the spatial patterns in morphometry (area, mean depth) and physicochemical characteristics (pH, T, DOC, DIC,  $\text{CH}_4$ , and Rn) of the ponds. Redundancy analysis (RDA) was used to identify the major variables of the ponds that explained the FA and SI patterns of chironomids and dytiscids. In the RDA, the model-building procedure started from the unconstrained model (i.e., without any environmental variable) and applied stepwise forward selection based on the Akaike's information criterion to choose the best model. ANOVA-like permutation tests were used to assess if the explanatory variables (i.e., constraints) were significant ( $p < 0.05$ ) at each step when a constraint was added. Variance inflation factors (VIFs) of the constraints were also checked, and only those that had low VIFs (i.e.,  $\leq 10$ ; Oksanen, 2017) were included. Our initial analysis showed that DOC, DIC, conductivity, and mean depth of the ponds had high VIFs. These variables were thus removed from the RDA model, even though they were selected based on forward selection. A permutation test was used to determine if the final model was statistically significant ( $p < 0.05$ ). We obtained the adjusted variance explained by the final model using the vegan function "RsquareAdj." All analyses were conducted using the packages stats and vegan in R software (version 3.3.3; R Core Team, 2017).

**Table 1**

*Physicochemical Parameters of Ponds Waters and Active Layer Groundwater: Conductivity (Cond), Dissolved Oxygen (DO), Dissolved Inorganic Carbon (DIC), Total Nitrogen (TN), Methane (CH<sub>4</sub>), Carbon Dioxide (CO<sub>2</sub>), and Radon (Rn)*

Code	Type	Area (m <sup>2</sup> )	Mean depth (m)	Temp (°C)	pH	Cond (μS cm <sup>-1</sup> )	DO	DOC	DIC	TN	CH <sub>4</sub>	CO <sub>2</sub>	Rn (Bq m <sup>-3</sup> )
							(mg L <sup>-1</sup> )						
SF1	Pond	19.8	0.21	16.8	4.4	45.2	2.5	54.8	12	1.5	0.34	4.4	35 ± 18
SF2	Pond	32.4	0.21	16.4	4.8	31.9	3.8	67.9	16	2.7	0.33	3.3	56 ± 22
SF3	Pond	26.0	0.46	12.4	5.9	46.0	3.8	21.0	21	0.6	2.11	32.0	300 ± 48
SF4	Pond	44.5	0.71	12.4	5.9	40.6	1.7	25.4	15	0.7	0.79	44.6	703 ± 75
SF5	Pond	15.2	1.06	12.8	6.1	41.9	3.7	23.7	11	0.7	0.09	30.3	726 ± 74
SD1	Pond	30.2	0.61	12.3	4.5	20.3	11.4	25.7	9	0.6	0.06	2.5	830 ± 77
SD2	Pond	65.9	0.46	13.7	6.6	29.5	5.1	7.2	7	0.3	0.07	4.4	736 ± 75
SD3	Pond	76.3	0.65	14.0	6.4	31.7	9.3	10.7	9	0.4	0.41	8.0	688 ± 75
SD4	Pond	78.6	0.90	13.7	6.1	35.1	8.8	6.7	9	0.3	0.12	8.8	472 ± 58
SD5	Pond	36.9	0.44	12.3	4.4	26.7	4.3	46.9	9	1.5	0.23	9.9	577 ± 67
GW-SF	Well	-	-	-	N.A.	N.A.	N.A.	228	49	13.0	9.00	N.A.	384 ± 114
GW-SD1	Well	-	-	-	N.A.	N.A.	N.A.	64	11	2.2	0.28	N.A.	249 ± 79
GW-SD2	Well	-	-	-	N.A.	N.A.	N.A.	41	8	1.7	0.11	N.A.	230 ± 80
GW-SF-2	Bore	-	-	-	N.A.	N.A.	N.A.	N.A.	N.A.	N.A.	N.A.	N.A.	350 ± 98
GW-SF-3	Bore	-	-	-	N.A.	N.A.	N.A.	N.A.	N.A.	N.A.	N.A.	N.A.	451 ± 112
GW-SF1	Bore	-	-	-	-	-	-	-	-	-	-	-	58 ± 23
GW-SF2	Bore	-	-	-	-	-	-	-	-	-	-	-	131 ± 24
GW-SF3	Bore	-	-	-	-	-	-	-	-	-	-	-	169 ± 35
GW-SF4	Bore	-	-	-	-	-	-	-	-	-	-	-	124 ± 32
GW-SF5	Bore	-	-	-	-	-	-	-	-	-	-	-	136 ± 33
GW-SD3	Bore	-	-	-	-	-	-	-	-	-	-	-	19 ± 21
GW-SD4	Bore	-	-	-	-	-	-	-	-	-	-	-	6 ± 17
GW-SD5	Bore	-	-	-	-	-	-	-	-	-	-	-	177 ± 25
GW-A	Bore	-	-	-	3.6	112	N.A.	106	27	2.1	0.10	N.A.	32 ± 34
GW-B	Bore	-	-	-	4.5	38	N.A.	54	26	1.6	0.01	N.A.	161 ± 78
GW-D	Bore	-	-	-	4.0	57	N.A.	97	43	2.1	1.80	N.A.	228 ± 107
GW-SF1	Bore	-	-	-	4.0	60	N.A.	85	27	2.8	0.78	N.A.	307 ± 125
GW-SF3	Bore	-	-	-	4.0	53	N.A.	73	29	1.5	1.50	N.A.	197 ± 87
Incub-D	Incub.	-	-	-	-	-	-	-	-	-	-	-	1715 ± 405
Incub-SF3	Incub.	-	-	-	-	-	-	-	-	-	-	-	1111 ± 490

### 3. Results

#### 3.1. Pond Physicochemical Characteristics

All study ponds were shallow, with mean depths ( $0.6 \pm 0.1$ , mean  $\pm$  standard deviation [sd]) that did not differ between the two mires ( $F = 0.20$ ,  $p = 0.67$ ). Ponds in Stordalen were generally larger (surface area of  $58 \pm 22$  m<sup>2</sup>) than those in Storflaket ( $28 \pm 11$  m<sup>2</sup>;  $F = 7.02$ ,  $p < 0.05$ ). Although there were differences in surface area, all ponds had similar morphology, as shown by their similar surface area to mean depth ratios ( $F = 0.55$ ,  $p = 0.48$ ) (Table 1).

Radon concentrations in pond waters ranged from 35 to 830 Bq m<sup>-3</sup>. Higher Rn concentrations were found in Stordalen ( $660 \pm 139$  Bq m<sup>-3</sup>) compared to Storflaket ( $364 \pm 337$  Bq m<sup>-3</sup>), although the differences were not significant ( $F = 3.3$ ,  $p = 0.11$ ) (Table 1). All ponds were DOC-rich ( $>5$  mg DOC L<sup>-1</sup>) and had CH<sub>4</sub>



concentrations (range of 0.1–2.1 mg L<sup>-1</sup>) well-above the air-equilibrium value (global atmosphere pCH<sub>4</sub> average of 1.8 μatm, Dlugokencky et al., 2009; Table 1), with no differences between mires (DOC:  $F = 2.4$ ,  $p = 0.16$ ; CH<sub>4</sub>:  $F = 0.18$  and  $p = 0.18$ ). Higher DIC concentrations, however, were measured in Storflaket (15 ± 4 mg L<sup>-1</sup>) compared to Stordalen (9 ± 1 mg L<sup>-1</sup>;  $F = 12.2$ ,  $p < 0.01$ ). On the contrary, higher DO values were observed in Stordalen (8 ± 3 mg L<sup>-1</sup>) compared to Storflaket (3 ± 1 mg L<sup>-1</sup>;  $F = 11.1$ ,  $p < 0.05$ ). No differences between sites were observed for temperature, pH, and TN concentrations ( $F = 1.7$ ,  $p > 0.01$ ). Higher conductivity was measured in Storflaket ponds ( $F = 12.3$ ,  $p < 0.05$ ).

### 3.2. Active Layer Groundwater

Groundwater from the active layer could not be easily sampled from the bores due to the low hydraulic conductivity of the peat at the sampled locations and the low amount of water collected from the installed piezometers. The low Rn enrichment (6–451 Bq m<sup>-3</sup>) in bore samples compared to surface waters was likely due to some Rn diffusion to the atmosphere during extraction. Higher Rn concentrations were obtained from sediment equilibration experiments (1,111–1,715 Bq m<sup>-3</sup>), with values that were at least 10 times higher than those measured in pond waters. The higher Rn concentrations in equilibrium with sediments likely resulted from Rn production from its parent Ra present in the sediments and the lack of atmospheric evasion and mixing with surface waters. For this study, we used the highest equilibration Rn concentration (1,715 ± 405 Bq m<sup>-3</sup>) as our active layer groundwater endmember. Our calculations may underestimate the actual active layer groundwater flows discharging into the thaw ponds, because using the highest estimated Rn concentration in groundwater is more conservative than using the mean value as the active layer end-member.

Concentrations of dissolved CH<sub>4</sub> in the active layer (range: 0.1–9.0 mg L<sup>-1</sup>) were up to two times higher than those measured in pond waters. Similarly, DOC (41–228 mg L<sup>-1</sup>) and TN (1.5–13.0 mg L<sup>-1</sup>) concentrations were significantly higher in the active layer relative to the ponds waters. In contrast, concentrations of DIC (range = 6.7–21 mg L<sup>-1</sup>) were within the range measured in the ponds waters. As CH<sub>4</sub> production and Rn concentrations in the active layer may vary at a fine scale (Paytan et al., 2015; Waddington & Roulet, 2000), we chose the concentration of CH<sub>4</sub> (1.8 mg L<sup>-1</sup>) measured at the same site where the sediments for incubations were collected as representative of our active layer groundwater end-member.

### 3.3. Groundwater-derived Inputs of CH<sub>4</sub> From the Active Layer to Thaw Ponds

The Rn mass balance equation (Equation 1) was solved analytically for each pond to obtain the amount of groundwater discharging from the active layer ( $Q_{gw}$ ). Uncertainties of individual terms were included in the estimation of the associated error (Figure S1; ISO, 1995; Taylor & Kuyatt, 1994). The values used to estimate all terms in Equation 1 are summarized in Table 2. An uncertainty assessment related to the determination of the groundwater discharge flows is provided in the Supporting Information (see Section S1 and Table S1).

The loss of Rn to the atmosphere ( $F_{atm}$ ) was determined using Equation 2. We assumed that atmospheric Rn concentration was negligible relative to Rn concentrations in the ponds waters ( $C_{Rn,air} = 0$ ). Using the hourly wind speed data for 24 h prior sampling resulted in normalized gas transfer velocities ( $k_{600}$ ) from 0.62 to 0.70 m day<sup>-1</sup>. Resulting losses of Rn to the atmosphere ranged from 29 to 345 Bq m<sup>-2</sup> day<sup>-1</sup>. Mean Rn losses due to decay were 61 ± 43 Bq m<sup>-2</sup> day<sup>-1</sup>. Of the combined Rn sinks, decay accounted for 7%–29%, while atmospheric exchange was 71%–93% of the total Rn losses (Figure S1).

Estimated diffusive Rn flux from underlying sediments ( $F_{diff}$ ) was 10 ± 2 Bq m<sup>-2</sup> day<sup>-1</sup>. For most of the ponds, the diffusive Rn flux could account only for 2%–7% of the total Rn sources. Only two ponds, SF1 and SF2, had a higher contribution, with diffusive Rn fluxes that accounted for 34% and 54% of all Rn sources, respectively. Since SF1 and SF2 were the shallowest ponds (ca. 0.2 m depth), their higher sediment area to water volume ratio compared to deeper ponds likely explains the higher contribution of diffusion to the total Rn pools. Due to the low concentrations of dissolved Ra in pond waters ( $[1.3 ± 1.1] × 10^{-5}$  Bq m<sup>-3</sup>), the production of Rn from Ra decay in the water column ( $[1.4 ± 1.3] × 10^{-5}$  Bq m<sup>-2</sup> day<sup>-1</sup>) was considered negligible in the Rn mass balance. Together, groundwater discharging from the active layer must be the hidden source that compensate for all Rn losses (Figure S1).

**Table 2**  
Definition of the Terms and Values Used in the Rn Mass Balance Based on Equation 1

Term	Definition	Pond					Unit
		SF1	SF2	SF3	SF4	SF5	
<b>Radon balance</b>							
$Rn_{gw}$	Rn concentration in active layer groundwater	172 ± 41	172 ± 41	172 ± 41	172 ± 41	172 ± 41	10 Bq m <sup>-3</sup>
$Ra_{pond}$	Ra concentration in pond water	21 ± 1	21 ± 1	21 ± 1	21 ± 1	21 ± 1	Bq m <sup>-3</sup>
$Rn_{pond}$	Rn concentration in pond water	35 ± 18	56 ± 22	300 ± 48	703 ± 45	726 ± 74	Bq m <sup>-3</sup>
$\lambda$	Rn decay constant	0.181	0.181	0.181	0.181	0.181	day <sup>-1</sup>
<b>Rn fluxes</b>							
$\lambda C_{Ra}V$	Rn production from Ra decay	1.6 ± 0.8	26 ± 1	45 ± 2	120 ± 6	61 ± 3	10 <sup>-1</sup> Bq day <sup>-1</sup>
$F_{diff}A$	Rn diffusion from sediments	210 ± 53	345 ± 86	276 ± 69	473 ± 119	161 ± 40	Bq day <sup>-1</sup>
$F_{atm}A$	Rn evasion to the atmosphere	36 ± 19	96 ± 38	354 ± 56	1436 ± 153	519 ± 53	10 Bq day <sup>-1</sup>
$\lambda C_{Ra}V$	Rn loss by decay	3 ± 1	7 ± 2	64 ± 4	3994 ± 11	2089 ± 5	10 Bq day <sup>-1</sup>
$Q_g C_g$	Rn flux from groundwater	18 ± 20	68 ± 39	390 ± 57	1787 ± 154	711 ± 53	10 Bq day <sup>-1</sup>
$Q_{gw}$	<b>Active layer groundwater flow</b>	<b>1 ± 1</b>	<b>4 ± 2</b>	<b>23 ± 3</b>	<b>104 ± 9</b>	<b>41 ± 3</b>	<b>10<sup>-1</sup> m<sup>3</sup> day<sup>-1</sup></b>
Term	Definition	Pond					Unit
		SD1	SD2	SD3	SD4	SD5	
<b>Radon balance</b>							
$Rn_{gw}$	Rn concentration in active layer groundwater	172 ± 41	172 ± 41	172 ± 41	172 ± 41	172 ± 41	10 Bq m <sup>-3</sup>
$Ra_{pond}$	Ra concentration in pond water	21 ± 1	21 ± 1	21 ± 1	21 ± 1	21 ± 1	Bq m <sup>-3</sup>
$Rn_{pond}$	Rn concentration in pond water	830 ± 77	736 ± 688	688 ± 75	472 ± 58	577 ± 67	Bq m <sup>-3</sup>
$\lambda$	Rn decay constant	0.181	0.181	0.181	0.181	0.181	day <sup>-1</sup>
<b>Rn fluxes</b>							
$\lambda C_{Ra}V$	Rn production from Ra decay	70 ± 3	116 ± 6	189 ± 9	269 ± 14	61 ± 3	10 <sup>-1</sup> Bq day <sup>-1</sup>
$F_{diff}A$	Rn diffusion from sediments	321 ± 80	700 ± 175	810 ± 203	835 ± 209	392 ± 98	Bq day <sup>-1</sup>
$F_{atm}A$	Rn evasion to the atmosphere	1043 ± 97	2076 ± 213	2305 ± 250	1635 ± 202	872 ± 102	10 Bq day <sup>-1</sup>
$\lambda C_{Ra}V$	Rn loss by decay	273 ± 6	401 ± 10	613 ± 17	600 ± 24	167 ± 5	10 Bq day <sup>-1</sup>
$Q_g C_g$	Rn flux from groundwater	1284 ± 97	2406 ± 214	2835 ± 251	2148 ± 204	999 ± 102	10 Bq day <sup>-1</sup>
$Q_{gw}$	<b>Active layer groundwater flow</b>	<b>75 ± 6</b>	<b>140 ± 13</b>	<b>165 ± 15</b>	<b>125 ± 12</b>	<b>58 ± 6</b>	<b>10<sup>-1</sup> m<sup>3</sup> day<sup>-1</sup></b>

Notes. The active layer groundwater discharge flows estimated from the Rn mass balance are highlighted in bold. Rn concentrations in ponds waters and active layer groundwaters, Rn production from Ra decay, Rn diffusion from sediments, and Rn loss by decay are reported as mean ± standard deviation.

Active layer groundwater flows discharging into the study ponds ( $Q_{gw}$ , [m<sup>3</sup> day<sup>-1</sup>]) were obtained by dividing the net Rn influx (Bq m<sup>-2</sup> day<sup>-1</sup>) by the Rn concentration in the groundwater end-member. The estimated groundwater discharge flows ranged from 0.1 to 17 m<sup>3</sup> day<sup>-1</sup>. Only one pond (SF1) had almost non-detectable discharges (Table 2). This is likely due to the high contribution of sediment diffusion to the total Rn pools in this pond (Figure S1), which might have diluted the Rn signal from groundwater and hampered its quantification. The associated transport of CH<sub>4</sub> from the active layer was estimated by multiplying the groundwater discharge flow by the concentration of CH<sub>4</sub> in the groundwater end-member. Derived methane inputs (253 mg C m<sup>-2</sup> day<sup>-1</sup>, IQR: 142–307 mg C m<sup>-2</sup> day<sup>-1</sup>) were almost two times higher than the diffusive CH<sub>4</sub> emissions (122 mg C m<sup>-2</sup> day<sup>-1</sup>, IQR: 40–163 mg C m<sup>-2</sup> day<sup>-1</sup>; Figure 2).

### 3.4. Variation in Morphometric and Physicochemical Characteristics Among Ponds

Results of PCA showed that the first two axes, that is, PC1 and PC2, explained ca. 41% and 30%, respectively, of the total variance in morphometric and physicochemical characteristics of the ponds (Figure 3).

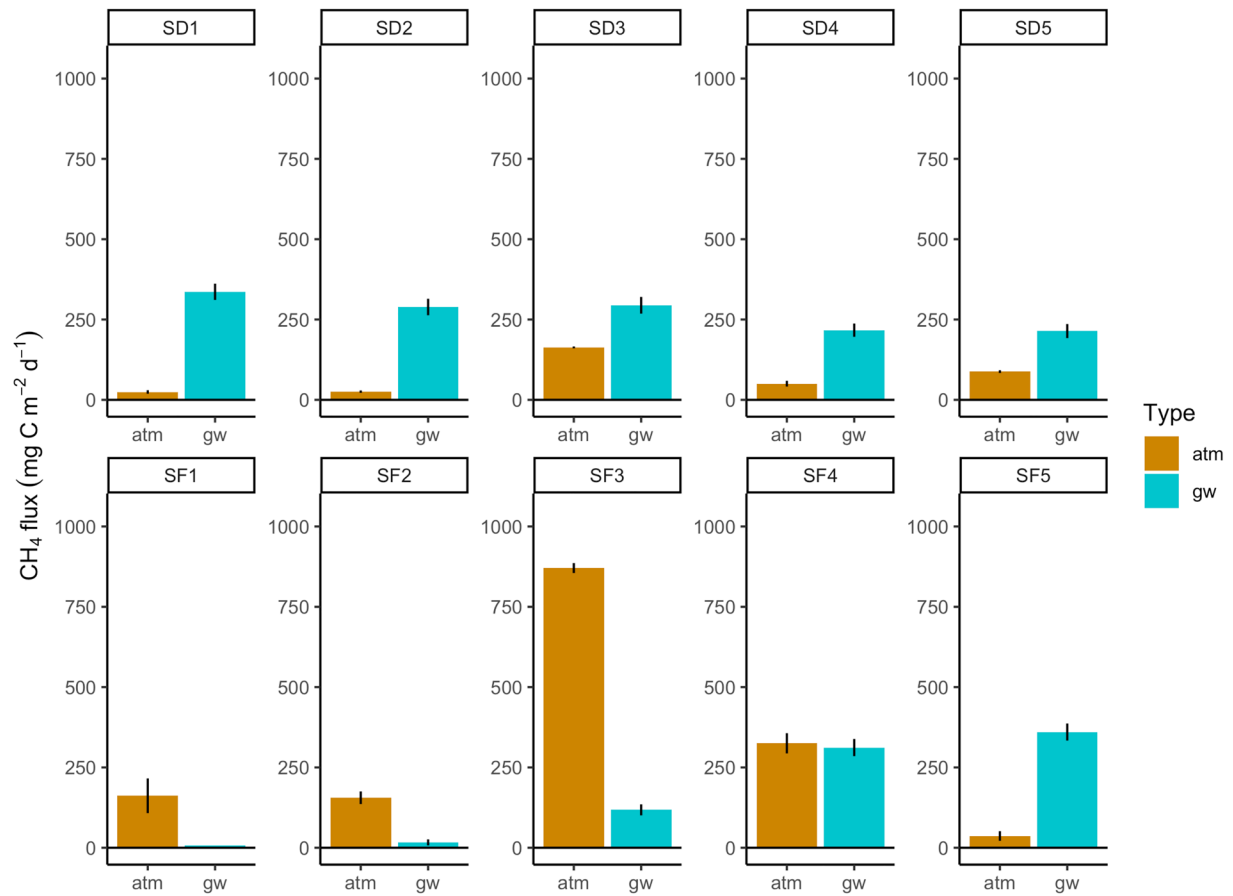


**Figure 2.** Diffusive CH<sub>4</sub> emissions and groundwater-mediated CH<sub>4</sub> inputs from the active layer in the study ponds. Error bars show the associated uncertainties derived from the Rn mass balance (see Supporting Information for details).

The pond morphometry was particularly explained by PC1. Shallower ponds (i.e., ponds with high surface area to sediment area ratio) had higher water temperatures and were characterized by lower pH, lower active layer groundwater discharge flows ( $Q_{gw}$ ), and by higher concentrations of DOC and TN (i.e., they were browner and more nutrient-rich). Gradients in these variables along PC1 were wider among ponds in Storflaket than in Stordalen. Ponds in Storflaket and Stordalen were particularly separated along PC2 that mainly correlated with DO, conductivity, CH<sub>4</sub>, CO<sub>2</sub>, and DIC. Ponds in Stordalen had higher DO than those in Storflaket (Table 1). In contrast, conductivity, CH<sub>4</sub>, CO<sub>2</sub>, and DIC were generally higher in Storflaket than in Stordalen. Groundwater discharge from the active layer was negatively correlated with DOC.

### 3.5. Benthic Fauna

Chironomid larvae were absent from one study pond (SF2) and dytiscids were absent from four ponds (SF3, SF4, SF5, and SD4; Table S2). Isotopic signatures of chironomid larvae varied among ponds, with their  $\delta^{13}C$  ranging from  $-37.3\text{‰}$  to  $-28.4\text{‰}$  in Storflaket, and from  $-32.1\text{‰}$  to  $-29.1\text{‰}$  in Stordalen. If excluding data from SF1, chironomid larvae at Storflaket were more  $^{13}C$ -depleted than those at Stordalen (Table S2). Chironomids had similar  $\delta^{15}N$  ranges in Storflaket (3.1–5.6‰) and Stordalen (1.7–5.1‰).  $\delta^{13}C$  and  $\delta^{15}N$  ranges of the predatory dytiscids (adults and/or larvae) were  $-32.5\text{‰}$  to  $-29.2\text{‰}$  and 2.3‰–5.3‰, respectively. In ponds where dytiscids were present, the  $\delta^{13}C$  of their prey chironomids were higher than  $-32\text{‰}$  (Table S2). Dytiscids had similar  $\delta^{13}C$  and  $\delta^{15}N$  as chironomids from the same ponds (Table S2). Chironomids tended to have higher molar C:N in Storflaket (range: 4.2–4.6) than in Stordalen (3.8–4.2), while dytiscids had similar C:N in the two mires (Storflaket: 4.5–5.2; Stordalen: 3.5–4.9).

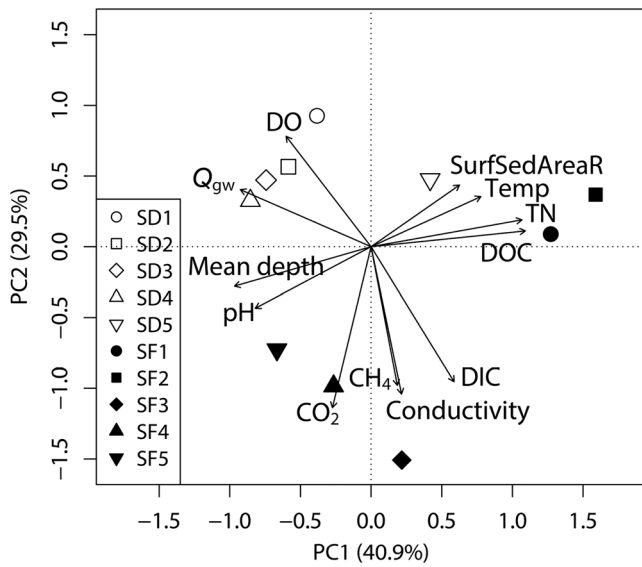


**Figure 3.** Principal component analysis of physicochemical characteristics of the study ponds. Percentages of variance explained by the principal component axes are given in parentheses.  $Q_{gw}$  and SurfSedAreaR refer to active layer groundwater discharge flows and surface area to sediment area ratios of the ponds, respectively. See Table 1 for other abbreviations.

Overall, chironomids and dytiscids in the ponds contained 7.8–66 and 17–65 mg total FA  $g^{-1}$  dry mass, respectively. In total 33 prevalent FA were identified, six of which were specific for bacteria (Table S2). The RDA results showed that the pond variables explained 59.0% (eigenvalue = 22.44; adjusted  $R^2 = 0.39$ ) of total variance in FA and SI of both chironomids and dytiscids (Figure 4). The first two RDA axes (i.e. RDA1 and RDA2) accounted for ca. 45% and 20% (eigenvalues = 10.08 and 4.43) of the explained variance, respectively. Chironomids and dytiscids appeared to differ in FA compositions and SI values, and form distinct groups along RDA1. Dytiscids were generally richer in both  $\omega 3$  (i.e.,  $\alpha$ -linolenic acid [ALA], eicosapentaenoic acid [EPA]) and  $\omega 6$  FA (i.e., linoleic acid [LIN], arachidonic acid [ARA]), and had higher  $\omega 3:\omega 6$  FA ratios and total FA concentrations compared to chironomids (Figure 4b). Yet, intraspecific variability in these FA responses were evident along RDA1. Chironomids and dytiscids were richer in ALA, EPA, LIN, ARA and total FA, and had higher  $\omega 3:\omega 6$  but lower concentrations of monounsaturated FA (i.e., 16:1 $\omega 7$ , 15:1 $\omega 5$ ) and bacterial FA (i.e., anteiso15:0, iso16:0), in ponds with higher temperatures and surface area to sediment area ratios, and with lower concentrations of  $CH_4$  and  $CO_2$  where lower activities of MOB were expected (Figures 4a and 4b).

Chironomids showed slightly greater variability than dytiscids along RDA2 (Figure 4a). In ponds with higher pH, DO, and groundwater discharge flows but lower TN concentrations, chironomids accumulated more docosahexaenoic acid (DHA) and long-chain saturated FA (i.e., 21:0, 22:0), but less oleic acid (OA) and short-chain saturated FA (i.e., 13:0). In ponds with higher  $CH_4$  concentrations and lower DO, chironomids had higher concentrations of short-chain saturated FA (i.e., 10:0, 12:0, 14:0, 15:0, 16:0), monounsaturated FA (i.e., 15:1 $\omega 5$ , OA), and bac-

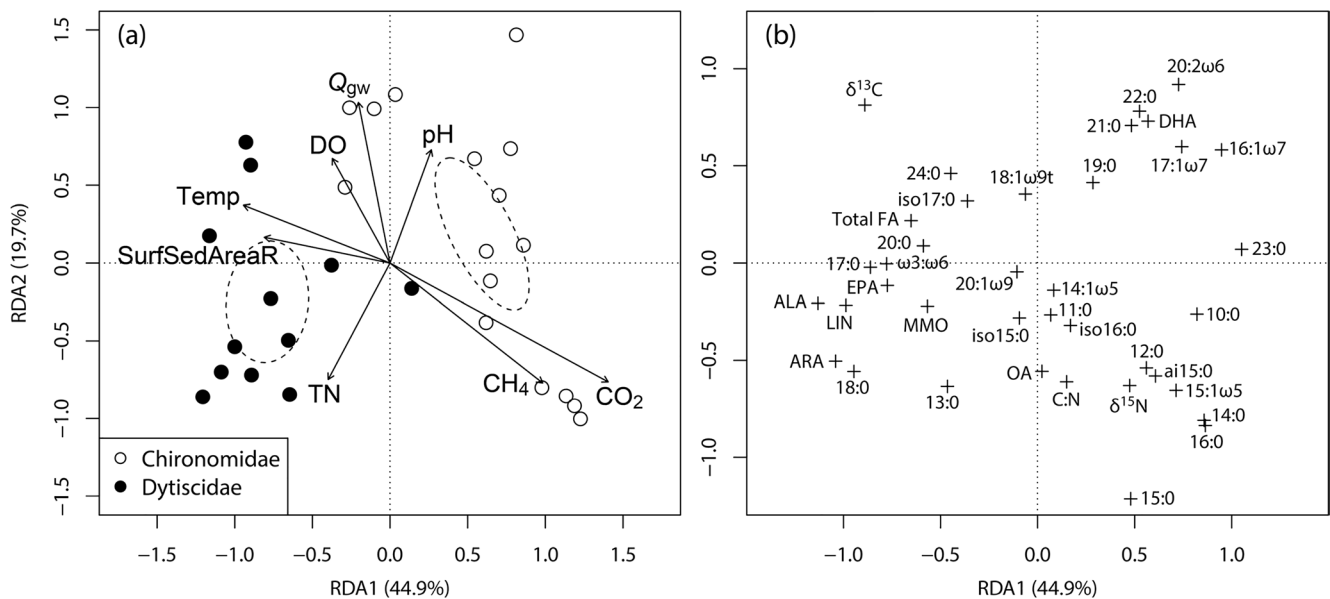


**Figure 4.** Redundancy analysis of dytiscid and larval chironomid fatty acids and stable isotopes. (a) Sample ordinations and significant explanatory variables (solid arrows; permutation tests:  $p < 0.05$ ). Ellipses indicate 95% confidence limits for individual taxa. (b) Fatty-acid and stable-isotope responses. Percentages of variance explained by the canonical axes are given in parentheses. Adjusted  $R^2$  of the model was 0.38.  $Q_{gw}$ , active layer flow; SurfSedAreaR, surface area to sediment area ratio; C:N, molar C:N ratio; ai15:0, anteiso15:0; MMO, methyl cis-9,10-methyleneoctadecanoate. See Table 1 and Table S2 for abbreviations of other environmental variables and FA.



terial FA such as anteiso15:0 and iso16:0. Chironomids in these systems also had higher C:N and were more  $^{15}\text{N}$ -enriched, but more  $^{13}\text{C}$ -depleted.

#### 4. Discussion

Our results showed that groundwater from the active layer was discharging into the study ponds, except for the shallowest (0.2 m deep) system (SF1). The associated inputs of terrestrially produced  $\text{CH}_4$  could sustain the total diffusive  $\text{CH}_4$  emissions from these systems (Figure 2), supporting our first prediction. The higher estimated diffusive  $\text{CH}_4$  flux found in one of the ponds (SF3) compared to the  $\text{CH}_4$  input from the active layer was likely due to an overestimation of the diffusive  $\text{CH}_4$  flux related to accidental bubble sampling. Also, chironomids and dytiscids had lower  $\delta^{13}\text{C}$  and higher  $\delta^{15}\text{N}$  in ponds with higher  $\text{CH}_4$  concentrations (Figure 4), indicating their greater trophic reliance on MOB. These consumer taxa appeared to differ in FA compositions. Yet, in both taxa the more  $^{13}\text{C}$ -depleted and  $^{15}\text{N}$ -enriched consumers had lower PUFA concentrations but higher tissue concentrations of short-chain saturated FA and bacterial FA (Table S2). These results support our second prediction and suggest that increasing trophic support from MOB had resulted in lower nutritional quality of the consumers and longer food chains.

##### 4.1. Significance of Groundwater Discharge From the Active Layer on the $\text{CH}_4$ Cycling of Subarctic Thaw Ponds

Similar to lakes and ponds in arctic and subarctic regions, the study ponds were supersaturated with  $\text{CH}_4$ , with diffusive  $\text{CH}_4$  emissions that varied up to one order of magnitude between ponds. As the weather conditions were similar in both Stordalen and Storflaket mires during the sampling (i.e., similar gas transfer velocities), the variability in the diffusive  $\text{CH}_4$  emissions likely reflects the spatial variation in  $\text{CH}_4$  concentrations of the ponds. This indicates the need for high spatial resolution measurements of  $\text{CH}_4$  concentrations for accurate estimates of  $\text{CH}_4$  emissions from these systems. Diffusive  $\text{CH}_4$  emissions from the study ponds ( $122 \text{ mg C m}^{-2} \text{ day}^{-1}$ , IQR:  $40\text{--}163 \text{ mg C m}^{-2} \text{ day}^{-1}$ ) were greater than the diffusive  $\text{CH}_4$  emissions estimated from three small lakes in Stordalen ( $5.2 \pm 0.3 \text{ mg C m}^{-2} \text{ day}^{-1}$ ; Jansen et al., 2020) as well as from larger and deeper lakes elsewhere within the same catchment ( $0.14 \pm 0.05 \text{ mg C m}^{-2} \text{ day}^{-1}$ , Lundin et al., 2016). Our estimates are at the high end of diffusive  $\text{CH}_4$  emissions reported from northern ( $>50^\circ\text{N}$  latitude) thermokarst water bodies (from  $3$  to  $38 \text{ mg C m}^{-2} \text{ day}^{-1}$ ; Wik et al., 2016) and thaw ponds in northern Canada (from  $0.4$  to  $192 \text{ mg C m}^{-2} \text{ day}^{-1}$ ; Laurion et al., 2010; McLaughlin & Webster, 2014). In line with the literature findings (Kuhn et al., 2018), our study indicates that small thaw ponds are significant sources of  $\text{CH}_4$  to the atmosphere.

As we predicted, groundwater discharge flows from the active layer were nontrivial, with values that ranged from 6% to 46% of pond volume per day. Estimates of the associated  $\text{CH}_4$  export revealed that active layer groundwater discharge constitutes an important source of  $\text{CH}_4$  to thaw ponds and can sustain the total  $\text{CH}_4$  emissions from these systems (Figure 2). As we used the same  $\text{CH}_4$  concentration for the end-member for all the ponds, the variability in groundwater-derived  $\text{CH}_4$  inputs observed here reflects the differences in the magnitude of the groundwater discharge between ponds rather than the differences in  $\text{CH}_4$  production within and between mires. Estimated terrestrial  $\text{CH}_4$  inputs from the active layer found here are higher than those found in Toolik Lake ( $1.2\text{--}8.4 \text{ mg C m}^{-2} \text{ day}^{-1}$  [Paytan et al., 2015]) and Landing Lake ( $24\text{--}96 \text{ mg C m}^{-2} \text{ day}^{-1}$  [Dabrowski et al., 2020]) in Alaska, primarily due to the greater magnitude of groundwater flows discharging into the study ponds ( $1\text{--}26 \text{ cm day}^{-1}$ ) compared to the Alaskan lakes ( $0.6\text{--}2.1 \text{ cm day}^{-1}$ ). The higher external inputs of  $\text{CH}_4$  found here may, in part, explain the higher  $\text{CH}_4$  concentrations in thaw ponds compared to larger systems such as lakes. Similarly, the estimated  $\text{CH}_4$  inputs from the active layer at Stordalen were similar to or even greater than the daily average  $\text{CH}_4$  bubble flux ( $15 \text{ mg C m}^{-2} \text{ day}^{-1}$ ) measured from nearby ponds in the same mire complex (Burke et al., 2019) and within the range reported for other surface water systems within the same catchment (from  $5$  to  $99 \text{ mg C m}^{-2} \text{ day}^{-1}$ ; T. Johansson et al., 2006; Wik et al., 2013). A similar range of ebullitive fluxes was found for northern ( $>50^\circ\text{N}$ ) thermokarst water bodies (from  $7$  to  $132 \text{ mg C m}^{-2} \text{ day}^{-1}$ ; Wik et al., 2016). The similar magnitude of groundwater-mediated  $\text{CH}_4$  inputs from the active layer with diffusive and ebullition  $\text{CH}_4$  fluxes found here highlights the need to consider active layer groundwater discharge as an important  $\text{CH}_4$  transport pathway in small thaw ponds.

As warming continues in the Arctic, the relative importance of active layer groundwater discharge on controlling CH<sub>4</sub> emissions from thaw ponds is likely to be stronger, because permafrost thawing will change hydrologic conditions and active layer thickness, likely increasing the amount of terrestrial dissolved C compounds into freshwaters (Walvoord & Kurylyk, 2016; Wrona et al., 2016).

#### 4.2. Influence of Active Layer Groundwater Discharge on the Trophic Chain in Subarctic Thaw Ponds

Methane inputs from the active layer through groundwater discharge were higher than the diffusive CH<sub>4</sub> emission rates (Figure 2), suggesting that most (9%–92%) of the terrestrially produced CH<sub>4</sub> was oxidized before being released to the atmosphere. This loss term is not surprising, as a high proportion (30%–94%) of the CH<sub>4</sub> produced in lake sediments can be oxidized at the sediment-water interface (Frenzel et al., 1990; Utsumi et al., 1998). In this way, CH<sub>4</sub> oxidation likely had counterbalanced, at least in part, some of the terrestrial inputs of CH<sub>4</sub> associated with the discharge of active layer groundwater. Vegetation at the pond margins might have also mediated the CH<sub>4</sub> fluxes by affecting both the production and the oxidation of CH<sub>4</sub>, with sedge- and moss-dominated ponds having the lowest diffusive CH<sub>4</sub> emissions (Kuhn et al., 2018). While this study was not designed to quantify the effects of pond vegetation on CH<sub>4</sub> emissions, previous work suggests that CH<sub>4</sub> oxidation rates are higher at shallow ponds dominated by mosses than those with vascular plants or extensive open-waters (Knoblauch et al., 2015).

In this study, CH<sub>4</sub> oxidation was likely stronger in ponds with higher CH<sub>4</sub> concentrations. This is reflected by the increased trophic support of MOB to both primary consumers (i.e., chironomid larvae) and predators (dytiscidae) in the more CH<sub>4</sub>-rich systems, and because CH<sub>4</sub> oxidation is positively related to the growth efficiency and production of MOB (Bastviken et al., 2003). We observed relatively low δ<sup>13</sup>C values in chironomid larvae in most of the ponds, and these values were particularly low in ponds with the highest CH<sub>4</sub> concentrations and emissions (i.e., SF3 and SF4; Table 1 and Table S2). These results are consistent with our prediction that chironomids had assimilated greater amounts of MOB—which are more <sup>13</sup>C-depleted than other basal resources (Jones & Grey, 2011)—in the more CH<sub>4</sub>-rich and oxygen-depleted ponds. Chironomid δ<sup>13</sup>C values observed in the study ponds were within the usual range of those observed in lakes worldwide (i.e., –40‰ to –20‰; Jones et al., 2008). Furthermore, the median C contribution from MOB to chironomids was estimated between 5% and 9% in lakes worldwide (Jones et al., 2008), suggesting that the chironomids larvae also likely received <10% trophic support from MOB. Yet, the δ<sup>13</sup>C values of chironomids were very similar to those of dytiscids in our study, indicating that the energy and C from MOB had been transferred to higher trophic levels, although dytiscids were absent in SF3 and SF4 (Table S2). The more <sup>13</sup>C-depleted consumers (especially chironomids) also had higher concentrations of short-chained saturated FA (i.e., 10:0, 12:0, 14:0, 15:0 and 16:0) and FA anteiso15:0 that are indicative of bacterial diet (Napolitano, 1999; Taipale et al., 2012), and had higher δ<sup>15</sup>N values that indicate higher trophic positions or more trophic steps starting from the basal resources (i.e., longer food chains). All these results support our second prediction that variation in trophic reliance of chironomid larvae and their predators on MOB is influenced by differences in CH<sub>4</sub> concentrations across ponds (Figure 3). Also, our SI and FA results corroborate that the effects of active layer groundwater discharge on the balance between CH<sub>4</sub> supply and oxidation are important for explaining the MOB support of the pond food chains.

Our results also support the idea that the tissue PUFA concentrations of consumers are reduced with increasing trophic reliance on MOB. In particular, the more <sup>13</sup>C-depleted consumers had lower ω3:ω6 FA ratios and lower concentrations of EPA and ARA that are necessary for animal growth and reproduction (Ahlgren et al., 2009). This was likely because consumer diets varied depending on the basal resource availability. Algae (including both phytoplankton and benthic algae) are able to biosynthesize PUFA de novo and thus contain high amounts of ω3 (e.g., EPA and DHA) and ω6 PUFA (Brett & Müller-Navarra, 1997). However, algal production and availability was likely limited in ponds with high CH<sub>4</sub> concentrations, as these ponds were also more DOC-rich with lower light availability (Karlsson et al., 2009; Seekell et al., 2015). Our results suggest that the shift in relative availability from algae to MOB across ponds was associated with an increased trophic reliance of consumers on MOB, which in turn reduced the consumers' nutritional quality (as measured by tissue PUFA concentrations). Also, the algal trophic support for consumers in the CH<sub>4</sub>- and DOC-rich ponds was possibly lower than that in lakes. This is because the EPA concentrations in chirono-

mids and dytiscids (range = 0.1%–1.9% of total FA) in our study were lower than those reported for both pelagic and benthic primary consumers and predators (3%–13% of total FA in general) in oligotrophic and humic boreal lakes (Lau et al., 2012), where reduced EPA concentrations in consumers are the result from lower trophic reliance on in-lake primary production (Lau et al., 2014). Hence, we conjecture that thaw ponds have more limited algal supply of essential PUFA for the aquatic food webs than do lake ecosystems.

The tissue concentrations of DHA (a FA important for neural tissue development; Ahlgren et al., 2009) in chironomids were positively correlated with the groundwater discharge from the active layer into the study ponds (Figure 3), but these values were generally low overall (<0.1% of total FA) and were consistent with the DHA levels in larval chironomids in boreal lakes (Goedkoop et al., 2000). This result suggests that chironomids may not be the main prey that transfer DHA to the pond predators (e.g., dytiscids), which usually require more DHA than do lower trophic level taxa (Ahlgren et al., 2009). Also, dytiscids were not found in ponds with higher CH<sub>4</sub> concentrations, potentially because these lacked suitable habitats (e.g., DO levels are too low), or because there was limited dietary PUFA support for the production of higher trophic levels (Lau et al., 2014). Finally, the lower PUFA trophic transfer in the aquatic food chains of CH<sub>4</sub>-rich ponds may also affect the surrounding terrestrial ecosystems. For instance, during the transition from larval to adult stages, chironomids emerge from ponds and become potential prey for terrestrial predators. Decreases in nutritional quality of chironomids will therefore also lower the dietary PUFA availability for the terrestrial predators (Martin-Creuzburg et al., 2017). As a result, changes in resource use and nutritional quality in relation to altered CH<sub>4</sub> inputs from the active layer and in-pond CH<sub>4</sub> oxidation could have wider ecological impact on the entire landscape.

## 5. Conclusions

Our study demonstrates that groundwater discharge from the active layer is an important mechanism for transporting terrestrially derived CH<sub>4</sub> into thaw ponds, and that this external CH<sub>4</sub> input can sustain the total CH<sub>4</sub> emissions from the thaw ponds. The external CH<sub>4</sub> supply was likely counterbalanced, at least in part, by CH<sub>4</sub> oxidation. The effects of active layer groundwater discharge on the balance between CH<sub>4</sub> inputs and oxidation will further impact the pond food chains. Our results suggest that increasing concentrations and/or oxidation of CH<sub>4</sub> will enhance the trophic reliance of pond consumers on MOB, consequently lowering their overall nutritional quality. Due to seasonal (limited to summer) and site-specific conditions, our findings should be extrapolated with caution to other arctic and subarctic regions. Nevertheless, widespread permafrost warming and increased precipitation are projected to alter the hydrology of the Arctic, likely increasing the influx of terrestrial CH<sub>4</sub> into inland waters. Accurate quantification of CH<sub>4</sub> inputs from the active layer through groundwater discharge and the consequent effects on the MOB-consumer interactions is thus necessary to improve predictions of CH<sub>4</sub> emissions from small thaw ponds.

### Acknowledgments

We are grateful to A. Lupon, V. Rodellas, and J. Karlsson for their helpful discussions and feedbacks in the manuscript. E. McCallum and R. Sponseller are thanked for their help with the final edits. We acknowledge E. Lundin for providing the map of the Stordalen catchment. The wind speed data has been made possible by data provided by Abisko Scientific Research Station and the Swedish Infrastructure for Ecosystem Science (SITES). We also thank the staff at the Abisko Scientific Research Station for logistic and technical support. We are grateful to Grup de Recerca de Radioactivitat Ambiental de Barcelona (GRAB) at Universitat Autònoma de Barcelona (UAB) for their help with the Rn analyses. C. Olid acknowledges financial support from Formas (Dnr 2018-01217). We would like to thank the two anonymous reviewers who gave useful comments on the manuscript.

### Conflict of Interest

The authors declare no conflict of interest relevant to this study.

### Data Availability Statement

Data will be available at Figshare Digital Repository (<https://figshare.com/s/77fda942b439f4ff3166>) or upon request from the corresponding author after the acceptance of the manuscript.

### References

- Ahlgren, G., Vrede, T., & Goedkoop, W. (2009). Fatty acid ratios in freshwater fish, zooplankton and zoobenthos—Are there specific optima? In M. T. Arts, M. Brett, & M. Kainz (Eds.), *Lipids in aquatic ecosystems* (pp. 147–178). New York, NY: Springer-Verlag. [https://doi.org/10.1007/978-0-387-89366-2\\_7](https://doi.org/10.1007/978-0-387-89366-2_7)
- Åkerman, H. J., & Johansson, M. (2008). Thawing permafrost and thicker active layers in sub-arctic Sweden. *Permafrost and Periglacial Processes*, 19(3), 279–292. <https://doi.org/10.1002/ppp.626>

- Alexandersson, H., Karlström, C., & Larsson-McCann, S. (1991). *Temperature and precipitation in Sweden 1961-90 reference normals SMHI Meteorologi Klimasektion (No. 81)*. Retrieved from <https://www.smhi.se/publikationer/temperaturen-och-nederborden-i-sverige-1961-90-referensnormaler-1.2441>
- Bastviken, D., Cole, J., Pace, M., & Tranvik, L. (2004). Methane emissions from lakes: Dependence of lake characteristics, two regional assessments, and a global estimate. *Global Biogeochemical Cycles*, 18, GB4009. <https://doi.org/10.1029/2004GB002238>
- Bastviken, D., Ejlertsson, J., Sundh, I., & Tranvik, L. (2003). Methane as a source of carbon and energy for lake pelagic food webs. *Ecology*, 84(4), 969–981. [https://doi.org/10.1890/0012-9658\(2003\)084\[0969:MAASOC\]2.0.CO;2](https://doi.org/10.1890/0012-9658(2003)084[0969:MAASOC]2.0.CO;2)
- Bastviken, D., Ejlertsson, J., & Tranvik, L. J. (2002). Measurements of methane oxidation in lakes: a comparison of methods. *Environmental Science & Technology*, 36(15), 3354–3361. <https://doi.org/10.1021/es010311p>
- Bouchard, F., Francus, P., Pienitz, R., Laurion, I., & Feyte, S. (2014). Subarctic thermokarst ponds: investigating recent landscape evolution and sediment dynamics in thawed permafrost of Northern Québec (Canada). *Arctic Antarctic and Alpine Research*, 46(1), 251–271. <https://doi.org/10.1657/1938-4246-46.1.251>
- Brett, M., & Müller-Navarra, D. (1997). The role of highly unsaturated fatty acids in aquatic foodweb processes. *Freshwater Biology*, 38(3), 483–499. <https://doi.org/10.1046/j.1365-2427.1997.00220.x>
- Burke, S. A., Wik, M., Lang, A., Contosta, A. R., Palace, M., Crill, P. M., & Varner, R. K. (2019). Long-term measurements of methane ebullition from thaw ponds. *Journal of Geophysical Research: Biogeosciences*, 124(7), 2018JG004786. <https://doi.org/10.1029/2018JG004786>
- Cable, J. E., & Martin, J. B. (2008). In situ evaluation of nearshore marine and fresh pore water radon activities via a single automated experiment. *Estuarine Coastal and Shelf Science*, 76(3), 473–483. <https://doi.org/10.1016/j.ECSS.2007.07.045>
- Callaghan, T. V., Bergholm, F., Christensen, T. R., Jonasson, C., Kokfelt, U., & Johansson, M. (2010). A new climate era in the sub-Arctic: Accelerating climate changes and multiple impacts. *Geophysical Research Letters*, 37(14), 1–6. <https://doi.org/10.1029/2009GL042064>
- Chanyo, S., Kranrod, C., & Burnett, W. C. (2014). Assessing diffusive fluxes and pore water radon activities via a single automated experiment. *Journal of Radioanalytical and Nuclear Chemistry*, 301, 581–588. <https://doi.org/10.1007/s10967-014-3157-3>
- Charette, M. A., Buesseler, K. O., & Andrews, J. E. (2001). Utility of radium isotopes for evaluating the input and transport of groundwater-derived nitrogen to a Cape Cod estuary. *Limnology and Oceanography*, 46(2), 465–470. <https://doi.org/10.4319/lo.2001.46.2.0465>
- Cole, J., & Caraco, N. (1998). Atmospheric exchange of carbon dioxide in a low-wind oligotrophic lake measured by. *Limnology and Oceanography*, 43(4), 647–656. <https://doi.org/10.4319/lo.1998.43.4.0647>
- Connolly, C. T., Bayani Cardenas, M., Burkart, G. A., Spencer, R. G. M., & McClelland, J. W. (2020). Groundwater as a major source of dissolved organic matter to Arctic coastal waters. *Nature Communications*, 11, 1479. <https://doi.org/10.1038/s41467-020-15250-8>
- Corbett, D. R., Burnett, W. C., Cable, P. H., & Clark, S. B. (1998). A multiple approach to the determination of radon fluxes from sediments. *Journal of Radioanalytical and Nuclear Chemistry*, 236(1–2), 247–253. <https://doi.org/10.1007/BF02386351>
- Crusius, J., & Wanninkhof, R. (2003). Gas transfer velocities measured at low wind speed over a lake. *Limnology and Oceanography*, 48(3), 1010–1017.
- Dabrowski, J. S., Charette, M. A., Mann, P. J., Ludwig, S. M., Natali, S. M., Holmes, R. M., et al. (2020). Using radon to quantify groundwater discharge and methane fluxes to a shallow, tundra lake on the Yukon-Kuskokwim Delta, Alaska. *Biogeochemistry*, 148, 69–89.
- DelSontro, T., del Giorgio, P. A., & Prairie, Y. T. (2018). No longer a paradox: The interaction between physical transport and biological processes explains the spatial distribution of surface water methane within and across lakes. *Ecosystems*, 21, 1073–1087. <https://doi.org/10.1007/s10021-017-0205-1>
- Dimova, N. T., Burnett, W. C., Chanton, J. P., & Corbett, J. E. (2013). Application of radon-222 to investigate groundwater discharge into small shallow lakes. *Journal of Hydrology*, 486, 112–122. <https://doi.org/10.1016/j.jhydrol.2013.01.043>
- Dlugokencky, E. J., Bruhwiler, L., White, J. W. C., Emmons, L. K., Novelli, P. C., Montzka, S. A., et al. (2009). Observational constraints on recent increases in the atmospheric CH<sub>4</sub> burden. *Geophysical Research Letters*, 36(18), 3–7. <https://doi.org/10.1029/2009GL039780>
- Frenzel, P., Thebrath, B., & Conrad, R. (1990). Oxidation of methane in the oxic surface layer of a deep lake sediment (Lake Constance). *FEMS Microbiology Letters*, 73(2), 149–158. <https://doi.org/10.1111/j.1574-6968.1990.tb03935.x>
- Gisnås, K., Etzelmüller, B., Lussana, C., Hjort, J., Sannel, A. B. K., Isaksen, K., et al. (2016). Permafrost map for Norway, Sweden and Finland. *Permafrost and Periglacial Processes*, 28(2), 359–378. <https://doi.org/10.1002/ppp.1922>
- Goedkoop, W., Sonesten, L., Ahlgren, G., & Boberg, M. (2000). Fatty acids in profundal benthic invertebrates and their major food resources in Lake Erken, Sweden: seasonal variation and trophic indications. *Canadian Journal of Fisheries and Aquatic Sciences*, 57(11), 2267–2279. <https://doi.org/10.1139/f00-201>
- Grieve, A., & Lau, D. C. P. (2018). Do autochthonous resources enhance trophic transfer of allochthonous organic matter to aquatic consumers, or vice versa? *Ecosphere*, 9(6). <https://doi.org/10.1002/ecs2.2307>
- Holgerson, M. A., & Raymond, P. A. (2016). Large contribution to inland water CO<sub>2</sub> and CH<sub>4</sub> emissions from very small ponds. *Nature Geoscience*, 9(3), 222–226. <https://doi.org/10.1038/ngeo2654>
- IPCC. (2013). *Climate Change 2013: The physical science basis*. Contribution of Working Group I to the fifth assessment report of the Intergovernmental Panel on Climate Change. Intergovernmental Panel on Climate Change, Working Group I Contribution to the IPCC Fifth Assessment Report (AR5) (p. 1535). New York, NY: Cambridge University Press.
- ISO. (1995). *Guide to Expression of Uncertainty in Measurement*. Geneva, Switzerland: International Organization for Standardisation.
- Jansen, J., Thornton, B. F., Cortés, A., Snöäl, J., Wik, M., MacIntyre, S., & Crill, P. M. (2020). Drivers of diffusive CH<sub>4</sub> emissions from shallow subarctic lakes on daily to multi-year timescales. *Biogeosciences*, 17, 1911–1932.
- Johansson, M., Callaghan, T. V., Bosio, J., Åkerman, H. J., Jackowicz-Korczynski, M., & Christensen, T. R. (2013). Rapid responses of permafrost and vegetation to experimentally increased snow cover in sub-arctic Sweden. *Environmental Research Letters*, 8(3), 035025. <https://doi.org/10.1088/1748-9326/8/3/035025>
- Johansson, T., Malmer, N., Crill, P. M., Friberg, T., Åkerman, J. H., Mastepanov, M., & Christensen, T. R. (2006). Decadal vegetation changes in a northern peatland, greenhouse gas fluxes and net radiative forcing. *Global Change Biology*, 12(12), 2352–2369. <https://doi.org/10.1111/j.1365-2486.2006.01267.x>
- Jones, R. I., Carter, C. E., Kelly, A., Ward, S., Kelly, D. J., & Grey, J. (2008). Widespread contribution of methane-cycle bacteria to the diets of lake profundal chironomid larvae. *Ecology*, 89(3), 857–864. <https://doi.org/10.1890/06-2010.1>
- Jones, R. I., & Grey, J. (2011). Biogenic methane in freshwater food webs. *Freshwater Biology*, 56, 213–229. <https://doi.org/10.1111/j.1365-2427.2010.02494.x>
- Karlsson, J., Byström, P., Ask, J., Ask, P., & Persson, L. (2009). Light limitation of nutrient-poor lake ecosystems. *Nature*, 460, 506–509. Retrieved from <http://www.nature.com/nature/journal/v460/n7254/abs/nature08179.html>
- Karlsson, J., Jansson, M., & Jonsson, A. (2007). Respiration of allochthonous organic carbon in unproductive forest lakes determined by the Keeling plot method. *Limnology and Oceanography*, 52(2), 603–608. <https://doi.org/10.4319/lo.2007.52.2.0603>



- Klaminder, J., Yoo, K., Rydberg, J., & Giesler, R. (2008). An explorative study of mercury export from a thawing palsa mire. *Journal of Geophysical Research*, *113*(4), 1–9. <https://doi.org/10.1029/2008JG000776>
- Kling, G. W., Kipphut, G. W., & Miller, M. C. (1992). The flux of CO<sub>2</sub> and CH<sub>4</sub> from lakes and rivers in Arctic Alaska. *Hydrobiologia*, *240*(1–3), 23–36. <https://doi.org/10.1007/BF00013449>
- Knoblauch, C., Spott, O., Evgrafova, S., Kutzbach, L., & Pfeiffer, E.-M. (2015). Regulation of methane production, oxidation, and emission by vascular plants and bryophytes in ponds of the northeast Siberian polygonal tundra. *Journal of Geophysical Research: Biogeosciences*, *120*(12), 2525–2541. <https://doi.org/10.1002/2015JG003053>
- Kuhn, M., Lundin, E. J., Giesler, R., Johansson, M., & Karlsson, J. (2018). Emissions from thaw ponds largely offset the carbon sink of northern permafrost wetlands. *Scientific Reports*, *8*(1), 9535–9537. <https://doi.org/10.1038/s41598-018-27770-x>
- Lau, D. C. P., Sundh, I., Vrede, T., Pickova, J., & Goedkoop, W. (2014). Autochthonous resources are the main driver of consumer production in dystrophic boreal lakes. *Ecology*, *95*(6), 1506–1519. <https://doi.org/10.1890/13-1141.1>
- Lau, D. C. P., Vrede, T., Pickova, J., & Goedkoop, W. (2012). Fatty acid composition of consumers in boreal lakes - variation across species, space and time. *Freshwater Biology*, *57*(1), 24–38. <https://doi.org/10.1111/j.1365-2427.2011.02690.x>
- Laurion, I., Vincent, W. F., MacIntyre, S., Retamal, L., Dupont, C., Francus, P., & Pienitz, R. (2010). Variability in greenhouse gas emissions from permafrost thaw ponds. *Limnology and Oceanography*, *55*(1), 115–133. <https://doi.org/10.4319/lo.2010.55.1.0115>
- Lecher, A. L., Chuang, P., Singleton, M., & Paytan, A. (2017). Sources of methane to an Arctic lake in Alaska: An isotopic investigation. *Journal of Geophysical Research: Biogeosciences*, *122*(4), 753–766. <https://doi.org/10.1002/2016JG003491>
- Lundin, E. J., Klaminder, J., Giesler, R., Persson, A., Olefeldt, D., Heliasz, M., et al. (2016). Is the subarctic landscape still a carbon sink? Evidence from a detailed catchment balance. *Geophysical Research Letters*, *43*, 1988–1995. <https://doi.org/10.1002/2015GL066970>
- MacIntyre, S., Wanninkhof, R., & Chanton, J. P. (1995). Trace gas exchange across the air-water interface in freshwaters and coastal marine environments. In P. A. Matson, & R. C. Harris (Eds.), *Biogenic trace gases: Measuring emissions from soil and water* (pp. 52–57). Blackwell.
- Malmer, N., Johansson, T., Olsrud, M., & Christensen, T. R. (2005). Vegetation, climatic changes and net carbon sequestration in a North-Scandinavian subarctic mire over 30 years. *Global Change Biology*, *11*, 1895–1909. <https://doi.org/10.1111/j.1365-2486.2005.01042.x>
- Martin-Creuzburg, D., Kowarik, C., & Straile, D. (2017). Cross-ecosystem fluxes: Export of polyunsaturated fatty acids from aquatic to terrestrial ecosystems via emerging insects. *Science of the Total Environment*, *577*, 174–182.
- McLaughlin, J., & Webster, K. (2014). Effects of climate change on peatlands in the far north of Ontario, Canada: A synthesis. *Arctic Antarctic and Alpine Research*, *1*, 84–102.
- Moore, W. S., & Reid, D. F. (1973). Extraction of radium from natural-waters using manganese-impregnated acrylic fibers. *Journal of Geophysical Research*, *36*, 8880–8886. <https://doi.org/10.1029/jc078i036p08880>
- Napolitano, G. E. (1999). Fatty acids as trophic and chemical markers in freshwater ecosystems. In M. T. Arts & B. C. Wainman (Eds.), *Lipids in freshwater ecosystems*, (pp. 21–44). New York, NY: Springer.
- O'Donnell, J. A., Jorgenson, M. T., Harden, J. W., McGuire, A. D., Kanevskiy, M. Z., & Wickland, K. P. (2012). The effects of permafrost thaw on soil hydrologic, thermal, and carbon dynamics in an Alaskan peatland. *Ecosystems*, *15*(2), 213–229. <https://doi.org/10.1007/s10021-011-9504-0>
- Oksanen, J. (2017). *Multivariate analysis of ecological communities in R: Vegan tutorial* (p. 39). Retrieved from <http://cc.oulu.fi/~jarioksa/opetus/metodi/vegantutor.pdf>
- Olefeldt, D., & Roulet, N. T. (2012). Effects of permafrost and hydrology on the composition and transport of dissolved organic carbon in a subarctic peatland complex. *Journal of Geophysical Research*, *117*(1), 1–15. <https://doi.org/10.1029/2011JG001819>
- Paytan, A., Lecher, A. L., Dimova, N., Sparrow, K. J., Kodovska, F. G.-T., Murray, J., et al. (2015). Methane transport from the active layer to lakes in the Arctic using Toolik Lake, Alaska, as a case study. *Proceedings of the National Academy of Sciences*, *112*(12), 201417392. <https://doi.org/10.1073/pnas.1417392112>
- Peterson, B. J., & Fry, B. (1987). Stable isotopes in ecosystem studies. *Annual Review of Ecology and Systematics*, *18*(1), 293–320. <https://doi.org/10.1146/annurev.es.18.110187.001453>
- R Core Team. (2017). *R: A language and environment for statistical computing*. R Foundation for Statistical Computing. Retrieved from <http://www.R-project.org/>
- Rodellas, V., Stieglitz, T. C., Andrisoa, A., Cook, P. G., Raimbault, P., Tamborski, J. J., et al. (2018). Groundwater-driven nutrient inputs to coastal lagoons: The relevance of lagoon water recirculation as a conveyor of dissolved nutrients. *The Science of the Total Environment*, *642*, 764–780. <https://doi.org/10.1016/j.scitotenv.2018.06.095>
- Rodellas, V., Stieglitz, T. C., Tamborski, J. J., van Beek, P., Andrisoa, A., & Cook, P. G. (2020). Conceptual uncertainties in groundwater and pore-water fluxes estimated by radon and radium mass balances. *Limnology and Oceanography*, *1*–19. <https://doi.org/10.1002/lno.11678>
- Rubbo, M. J., Cole, J. J., & Kiesecker, J. M. (2006). Terrestrial subsidies of organic carbon support net ecosystem production in temporary forest Ponds: Evidence from an ecosystem experiment. *Ecosystems*, *9*, 1170–1176. <https://doi.org/10.1007/s10021-005-0009-6>
- Schubert, M., Paschke, A., Lieberman, E., & Burnett, W. C. (2012). Air-water partitioning of 222Rn and its dependence on water temperature and salinity. *Environmental Science & Technology*, *46*, 3905–3911. <https://doi.org/10.1021/s204680n>
- Seekell, D. A., Lapiere, J.-F., Ask, J., Bergström, A.-K., Deininger, A., Rodriguez, P., & Karlsson, J. (2015). The influence of dissolved organic carbon on primary production in northern lakes. *Limnology and Oceanography*, *60*(4), 1276–1285. <https://doi.org/10.1002/lno.10096>
- Stieglitz, T. C., Beek, P. V., Souhaut, M., & Cook, P. G. (2013). Karstic groundwater discharge and seawater recirculation through sediments in shallow coastal Mediterranean lagoons, determined from water, salt and radon budgets. *Marine Chemistry*, *156*, 73–84. <https://doi.org/10.1016/j.marchem.2013.05.005>
- Taipale, S. J., Brett, M. T., Pulkkinen, K., & Kainz, M. J. (2012). The influence of bacteria-dominated diets on *Daphnia magna* somatic growth, reproduction, and lipid composition. *FEMS Microbiology Ecology*, *82*(1), 50–62. <https://doi.org/10.1111/j.1574-6941.2012.01406.x>
- Taylor, B. N., & Kuyatt, C. E. (1994). *Guidelines for Evaluating and Expressing the Uncertainty of NIST Measurement Results*. (NIST Tech. Note 1297). Washington, D.C.: U.S. Government Printing Office.
- Utsumi, M., Nojiri, Y., Nakamura, T., Nozawa, T., Otsuki, A., Takamura, N., et al. (1998). Dynamics of dissolved methane and methane oxidation in dimictic Lake Nojiri during winter. *Limnology and Oceanography*, *43*(1), 10–17. <https://doi.org/10.4319/lo.1998.43.1.0010>
- Vihma, T., Screen, J., Tjernström, M., Newton, B., Zhang, X., Popova, V., et al. (2016). The atmospheric role in the Arctic water cycle: A review on processes, past and future changes, and their impacts. *Journal of Geophysical Research: Biogeosciences*, *121*(3), 586–620. [https://doi.org/10.1002/2015JG003132%4010.1002/\(ISSN\)2169-8961.FRESHWATER1](https://doi.org/10.1002/2015JG003132%4010.1002/(ISSN)2169-8961.FRESHWATER1)
- Waddington, J. M., & Roulet, N. T. (2000). Carbon balance of a boreal patterned peatland. *Global Change Biology*, *6*, 87–97.

- Walter, K. M., Smith, L. C., & Stuart Chapin, F. (2007). Methane bubbling from northern lakes: Present and future contributions to the global methane budget. *Philosophical Transactions of the Royal Society A: Mathematical, Physical and Engineering Sciences*, 365(1856), 1657–1676. <https://doi.org/10.1098/rsta.2007.2036>
- Walvoord, M. A., & Kurylyk, B. L. (2016). Hydrologic impacts of thawing permafrost-A review. *Vadose Zone Journal*, 15(6), vjz2016.01.0010. <https://doi.org/10.2136/vzj2016.01.0010>
- Wanninkhof, R. (2014). Relationship between wind speed and gas exchange over the ocean revisited. *Limnology and Oceanography: Methods*, 12, 351–362. <https://doi.org/10.4319/lom2014.12.351>
- Wik, M., Crill, P. M., Varner, R. K., & Bastviken, D. (2013). Multiyear measurements of ebullitive methane flux from three subarctic lakes. *Journal of Geophysical Research: Biogeosciences*, 118(3), 1307–1321. <https://doi.org/10.1002/jgrg.20103>
- Wik, M., Varner, R. K., Anthony, K. W., MacIntyre, S., & Bastviken, D. (2016). Climate-sensitive northern lakes and ponds are critical components of methane release. *Nature Geoscience*, 9, 99–105. <https://doi.org/10.1038/ngeo2578>
- Woo, M.-K., Kane, D. L., Carey, S. K., & Yang, D. (2008). Progress in permafrost hydrology in the new millennium. *Permafrost and Periglacial Processes*, 19(2), 237–254. <https://doi.org/10.1002/ppp.613>
- Wrona, F. J., Johansson, M., Culp, J. M., Jenkins, A., Mård, J., Myers-Smith, I. H., et al. (2016). Transitions in Arctic ecosystems: Ecological implications of a changing hydrological regime. *Journal of Geophysical Research: Biogeosciences*, 121, 650–674. <https://doi.org/10.1002/2015JG003133>